Machining Science and Technology, 17:1–25

ISSN: 1091-0344 print/1532-2483 online
DOI: 10.1080/10910344.2012.747881

Taylor & Francis
Taylor & Francis Group

MATHEMATICAL MODELLING OF THE MECHANICS OF CORE DRILLING IN GEOMATERIALS

Bernardino Chiaia, Mauro Borri-Brunetto, and Alberto Carpinteri
Department of Structural, Geotechnical and Building Engineering, Politecnico di Torino, Torino, Italy

□ *A new, rational model is proposed for simulating the process of core drilling in geomaterials. The model describes in a consistent manner the complicated process of core drilling in quasi-brittle materials. After reviewing a model from the literature, based only on the balance of forces at the cutting edge, a new approach is introduced, considering a fundamental kinematical constraint to the rotary drilling process, namely, the helicoidal trajectories of the cutters. At the same time, the mechanical balance of engine power supply and drilling energy consumption must hold. The concept of drilling strength, i.e., the energy consumed to remove the unit volume of base material, is discussed, showing that the expression of the drilling strength depends on the fracture mechanisms occurring in the base material, and thus depends also on the shape of the indenters (back rake angle, wear-flat). A simple estimate of the wear effects at the cutting edges, based on experiments, is proposed. In conclusion, a global formulation of the core drilling process is obtained by coupling the kinematical and mechanical conditions. The model comprises a set of physical parameters, which can be determined according to drilling tests.*

Keywords core bits, drilling tools, theoretical models, wear

INTRODUCTION

There is an increasing demand for innovative tools able to drill into materials like reinforced concrete and hard rocks. However, research in the field has been limited, especially when compared to the wide literature concerning classical drilling tools for energy resources supply (e.g., in the field of petroleum engineering, see Kerr, 1988). Moreover, extending results from these fields to the process of core drilling into concrete and masonry must be done with much care, since the ploughing action of the indenters is, in some aspects, different from the traditional compressive

Address correspondence to Bernardino Chiaia, Department of Structural, Geotechnical and Building Engineering, Politecnico di Torino, Corso Duca degli Abruzzi 24, 10129, Torino, Italy. E-mail: bernardino.chiaia@polito.it

action on soils and rocks: although the physical processes are similar, and the sources of energy expenditure are the same in all geomaterials, the scaling ratio between the size of the indenter and the characteristic size of crystals, aggregates, and particles can be very different between artificial conglomerates and natural rocks. Neither can the theories of metal cutting be adopted when dealing with quasi-brittle materials, since plastic deformation is substituted by discontinuous chipping, fracture, and fragmentation (Chiaia, 2001).

A typical core drilling tool (Figure 1) is made of an electrical engine, a hollow cylindrical steel bit which can rotate at fixed power or at fixed angular velocity, and a series of indenters (or cutters) welded at the bottom of the bit, which penetrate into the base material and remove chips by a combined crushing/ploughing action. Two families of cutters for core drilling are available in the market, namely, the impregnated segments or the single hard indenters.

Impregnated segments (see, e.g., Miller and Ball, 1990, 1991) consist of a metal matrix where a distribution of small hard particles (usually synthetic diamonds) is embedded. Single indenters (Hanna, 2000; Sneddon and Hall, 1988) are made of hard metal (typically cemented tungsten carbide, WC-Co), and their cutting edge may be coated, for enhanced performance, with a layer of polycrystalline diamond (PCD). Although the

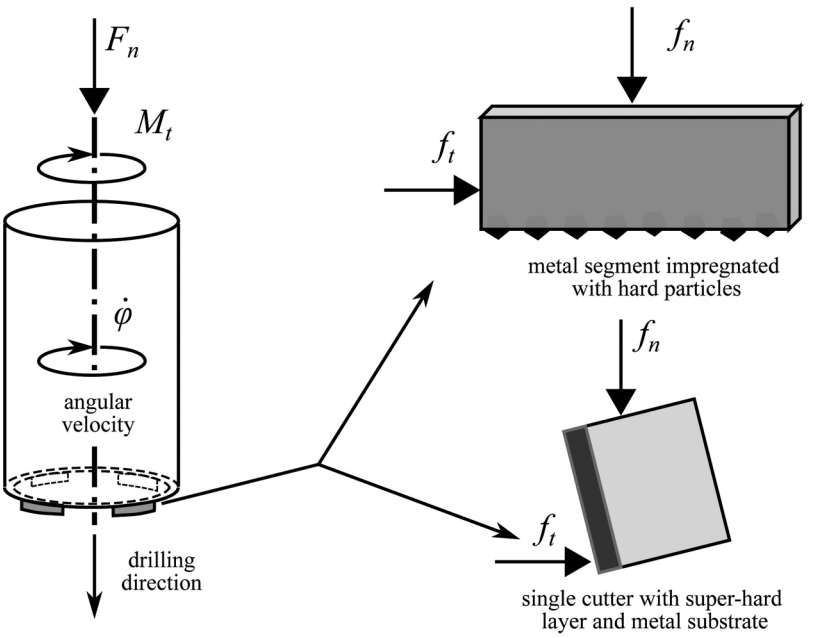

FIGURE 1 Schematic of a typical commercial tool for core drilling in concrete and masonry.

mechanical process is the same at the scale of the tool, the cutting action and the wear effects in the two cases are remarkably different at the scale of the cutters.

THE MODEL BY WOJTANOWICZ AND KURU

Assumptions of the Model

Wojtanowicz and Kuru (1993) derived a model for rock drilling, based on the static balance of the forces acting on a single cutter, assuming similarity between bit and cutter. Three equations constitute the mathematical model: torque, drilling velocity (or rate of penetration), and drill bit life. The equations consider cutter's geometry, rock properties, and five empirical constants, used to match the model to a real drilling process.

As shown in Figure 2, the model is derived from the analysis of the forces acting on each cutter, assuming that a certain wear-flat is already formed. In the model, u is the cutter penetration in the base material, θ is the cutting angle, β is the back rake angle, λ is the side rake angle, f_n and f_t are, respectively, the normal and tangential forces acting upon the indenter, f_c is the cutting force (orthogonal to the cutting area), f_w is the component of the normal force orthogonal to the wear-flat, f_{fw} and f_{fc} are the frictional forces acting respectively on the wear-flat area and on the cutting surface area. The bit life, drilling velocity, and bit torque equations are deduced from the balance of forces on a cutter moving with

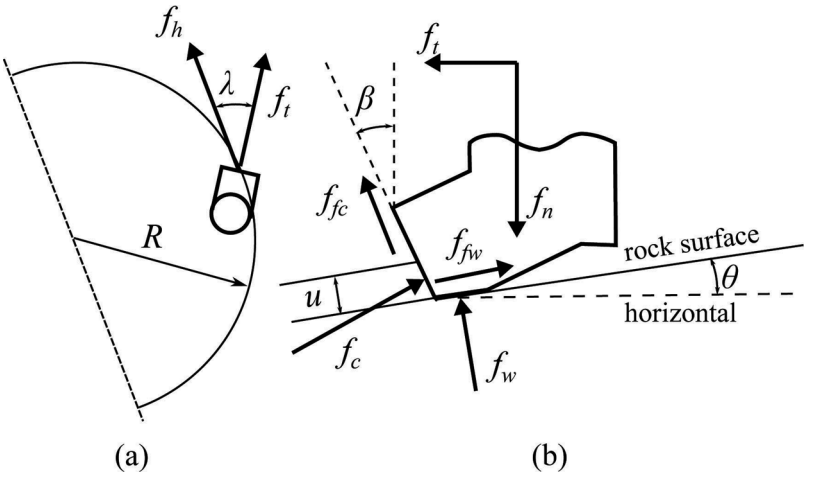

FIGURE 2 Geometrical and static assumptions according to Wojtanowicz and Kuru (1993): (a) axial view of the core bit; (b) lateral view of a cutter with back rake angle $\beta < 0°$.

constant angular velocity, $\dot{\varphi}$. The following assumptions are made throughout the derivation of the model:

1. The resistance to penetration and cutting is proportional to the contact area (i.e., the local normal force f_n upon each cutter does not depend on the penetration u).
2. There is perfect mechanical similarity between a single cutter and the bit. Thereby, experimental evidence claims for the following assumptions:
   - The advancement δ per bit rotation is proportional to the normal force f_n acting on a single cutter, with proportionality constant k_1.
   - The volumetric wear of the cutter is proportional to the work of friction at the contact area, with proportionality constant k_2. The frictional drag at the cutter's side surface is negligible.
   - The drilling velocity is proportional to the cutter penetration u, with proportionality constant k_3.
   - The bit torque M_t is proportional to the single cutter's torque, with proportionality constant k_4.
3. If the penetration is small, also the cutting angle θ is small and can be neglected in the balance of forces.

Force Balance Equations

The normal and tangential components of the forces acting on the cutter are:

$$f_n = -f_c\sin\beta + f_{fc}\cos\beta + f_w\cos\theta + f_{fw}\sin\theta \tag{1a}$$

$$f_t = f_c\cos\beta + f_{fc}\sin\beta - f_w\sin\theta + f_{fw}\cos\theta \tag{1b}$$

According to the assumptions described in the previous section, one can make the following substitutions:

$$f_c = S_c A_c \tag{2a}$$

$$f_w = S_w A_w \tag{2b}$$

$$f_{fc} = \mu f_c = \mu S_c A_c \tag{2c}$$

$$f_{fw} = \mu f_w = \mu S_w A_w \tag{2d}$$

where μ is the coefficient of friction between cutter and base material, S_c and S_w are the resistance to crushing and the resistance to penetration of the base material, respectively, $A_c = tu$ is the cutting area (t is the width of the groove), and A_w is the wear-flat area. This amounts to considering a

plastic response of the base material, with regard to both the vertical and the horizontal action of the cutter. No attention is paid to the penetration law (i.e., f_w does not depend on u). Inserting Equations (2) into the balance Equations (1), and taking $\theta \approx 0$, one obtains:

$$f_n = S_c A_c(\mu\cos\beta - \sin\beta) + S_w A_w \tag{3a}$$

$$f_t = S_c A_c(\cos\beta + \mu\sin\beta) + \mu S_w A_w \tag{3b}$$

Moreover, for typical values of the side rake angle, λ, smaller than 5°, the horizontal force f_h is practically coincident with the tangential force f_t (see Figure 2a):

$$f_h = \frac{f_t}{\cos\lambda} \approx f_t \tag{4}$$

Drilling Velocity Equation

The normal force balance equation can be solved for the cutting surface as:

$$A_c = \frac{f_n - S_w A_w}{S_c\ (\mu\cos\ \beta - \sin\beta)} \tag{5}$$

showing that the cutting area is a function of the cutter's penetration and of its wear state. Wear was considered by the authors through a dimensionless function U_D. Therefore, they obtained:

$$u = \frac{U_D\ (f_n - S_w A_w)}{t S_c(\mu\cos\beta - \sin\beta)} \tag{6}$$

As the drilling velocity $\dot{\delta}$ is proportional to u through an empirical constant k_3, if n_d is the number of cutters on the core bit, the bit progress per one full rotation is n_d-fold greater than u. Thus, the drilling velocity is given by:

$$\dot{\delta} = k_3 \dot{\varphi}^{k_5} n_d u \tag{7}$$

where k_5 is an exponent (close to 1.0) accounting for possible nonlinearities due to inadequate bottomhole cleaning. Substituting Equation (6) into Equation (7) and considering proportionality between total thrust (load on the bit) and cutter's normal force, we obtain $k_1 = n_d$. Thus, $F_n = k_1 f_n = n_d f_n$, and the drilling velocity equation becomes:

$$\dot{\delta} = k_3 \dot{\varphi}^{k_5} \frac{U_D(F_n - n_d S_w A_w)}{t S_c(\mu\cos\beta - \sin\beta)} = K(F_n - F_0) U_D \dot{\varphi}^{k_5} \tag{8}$$

where $F_0 = n_d S_w A_w$ and K is the *drillability constant*, defined as:

$$K = \frac{k_3}{tS_c(\mu\cos\beta - \sin\beta)} \tag{9}$$

According to this model, *both the drillability constant and the drilling velocity are independent of* n_d. We will see that the role of n_d does not come into play because of neglecting the nonlinearity of the penetration law.

HELICOIDAL MODEL FOR ROTARY DRILLING IN GEOMATERIALS

Kinematic Assumptions

The hypothesis of (circular) horizontal trajectories of the cutters, although acceptable at the level of force balance at the cutting edge, hinders important aspects of the core drilling process. In particular, it is impossible to model a continuous process, because, after each revolution in the horizontal plane (orthogonal to the z axis), a discontinuous axial advancement is required to allow the cutters to plough on. Moreover, because of the rotational symmetry, the horizontal trajectories would imply either that each cutter belonging to a trajectory of radius R works only for a small distance s (corresponding to the circumferential separation distance between two cutters, see Figure 3a), or that a single cutter removes the material for the entire loop, while all the others are shaded and do not work (Figure 3b).

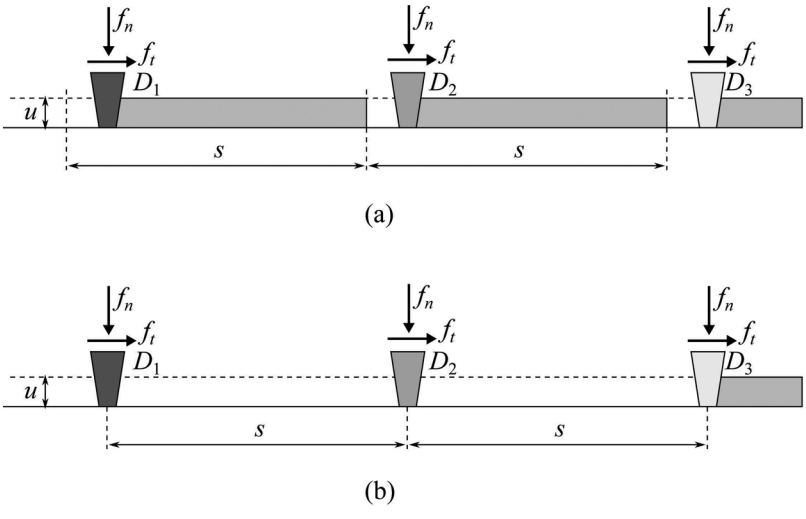

FIGURE 3 Horizontal trajectories of the indenters: (a) partial ploughing; (b) shadowing of cutters.

In order to model a continuous, stationary process and to respect the rotational symmetry (no cutter prevails over the others), it is necessary to consider *intersecting helicoidal trajectories* (Mellor, 1976). Each cutter is subjected to a normal component f_n (due to the penetration) and to a tangential one f_t (the cutting force) due to the ploughing action. Given two cutters D_1 and D_2 in a core bit with radius R, at a distance $s = 2\pi R/2$ (Figure 4), we can reasonably assume that, if the core bit is infinitely rigid compared to the base material, the two indenters are always at the same height z. Let us consider a clockwise rotation $\varphi = \pi$ (equal to the mutual angular separation between the indenters) and let δ be the vertical advancement. The indenters, at the end of the helicoidal motion, belong to the same horizontal plane. The *pitch* of the helix is related to the angle θ (the cutting angle), which can be considered as a measure of the rate of advancement (i.e., of the drilling velocity $\dot{\delta}$). We can generalize the process to an arbitrary number n_d of cutters, equally spaced within the circumference with radius R: their mutual distance s will be

$$s = \frac{2\pi R}{n_d} \tag{10}$$

Let us suppose that the penetration u is the same for all the cutters; this assumption is quite reasonable in a stationary regime, due to progressive wear of the indenters. One can immediately notice that, for a given value of δ, each cutter, when reaching the position previously occupied by the preceding cutter (i.e., after a rotation equal to $2\pi/n_d$), faces an obstacle of height δ. In particular, two situations may occur (Figure 5).

If $\delta < u$, each cutter would experience a decrease of its penetration when occupying the position previously occupied by another cutter (Figure 5a). This can only occur by decreasing the normal force, and would imply reduced drilling efficiency, tending in the limit to a mere polishing activity.

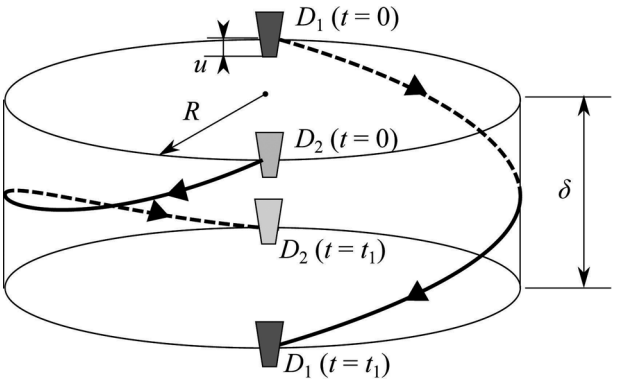

FIGURE 4 Helicoidal trajectories of the indenters.

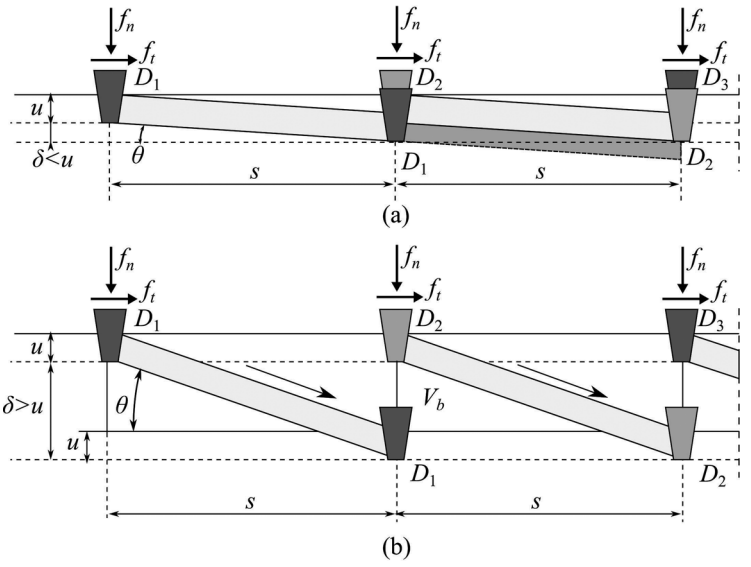

FIGURE 5 Non-stationary drilling situations: decreasing (a) or increasing drilling velocity (b).

On the contrary, if $\delta > u$, a certain volume of base material V_b has not been removed by the preceding cutters (Figure 5b). Thus, each cutter would face an obstacle higher than its penetration and this would imply an *increase* of its penetration, which is possible only by increasing the normal force. Both situations are cases of non-stationary drilling, i.e., Figure 5a refers to decreasing drilling velocity; whereas Figure 5b to increasing drilling velocity. These conditions are not consistent with an optimal and stationary drilling process. In particular, the case when $\delta > u$ represents a source of anomalous vibrations of the tool, due to the stick-slip behavior of the indenters. Moreover, wear of the cutters is extremely accelerated by these large fluctuations of the cutting force.

Thus, the rate of advancement θ, under steady-state conditions, must obey a strong kinematic restriction: the optimal value, $\bar{\theta}$, corresponds to the condition $\delta = u$, or, in other words, *each cutter must continuously face an obstacle of height exactly equal to its penetration* (Figure 6). In this way, the rotary

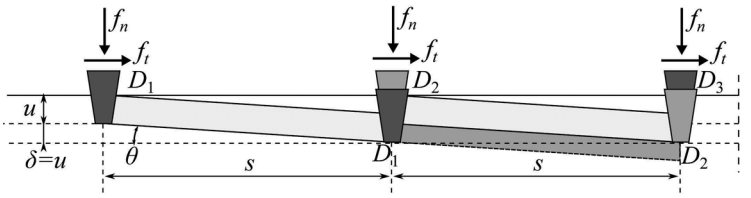

FIGURE 6 Optimal stationary kinematics of the drilling process.

process for each indenter becomes continuous, and the rotational symmetry is preserved. The optimal value of the cutting angle, $\bar{\theta}$, is directly related to the penetration and to the mutual distance among the cutters:

$$\tan \bar{\theta} = \frac{u}{s} \tag{11}$$

The apparently strange conclusion is that *the rate of advancement θ depends on the base material only by means of the penetration u.* The helicoidal advancement is controlled by kinematical quantities. The smaller the separation distance (in the direction of the motion) among the cutters (i.e., the larger the number of active cutters), the larger *must be* the advancement, for a given penetration, to ensure a stationary efficient process. Note, incidentally, that the presence of a larger number of active cutters requires a larger thrust on bit (and thus a larger value of the active torque M_t) to keep a certain value of the penetration u.

Kinematic Determination of the Drilling Velocity

By means of the above-mentioned geometrical arguments, the optimal kinematic conditions for the drilling velocity $\dot{\delta}$ can be obtained. We still need, however, to find the dependence of u on the total normal force F_n. Given the tangential velocity of the cutters, $\dot{\varphi}R$, the drilling velocity is:

$$\dot{\delta} = \dot{\varphi}R \tan \bar{\theta} = \frac{u}{s}\dot{\varphi}R = un_d\frac{\dot{\varphi}}{2\pi} \tag{12}$$

where we have used Equations (10) and (11). Notice the remarkable similarity between Equation (12) and Equation (7), obtained by Wojtanowicz and Kuru (1993) by means of empirical assumptions. The optimal rate of advancement $\bar{\theta}$ depends on the base material by means of the indenters' penetration u. One could argue that the larger the number of indenters, the larger the advancement rate, to ensure a stationary efficient process. However, a larger number of active indenters, *at fixed normal force F_n*, imply a smaller penetration u, and therefore the global effect of n_d remains to be explicated.

Let us consider now the following general penetration law for a single indenter:

$$f_n = ku^{\alpha} \tag{13}$$

where f_n is the normal force upon the indenter, and k, α are two constants depending on the base material, on the indenter geometry and on the wear state. As is well known in mechanics, the value $\alpha \approx 2$ is valid for elasto-plastic

indentation of cones and pyramids. It can be used for each small indenter embedded into an impregnated segment, but is not valid for the penetration of the whole cutter, since the total contact area is not constant. In the presence of large single hard indenters, the situation is closer to a *two-dimensional wedge*, with a linear load-penetration law in the elastic regime (Fischer-Cripps, 2000).

As regards the base material, we may argue that exponents $\alpha > 1$ should be used for very hard base materials, whereas, when F_n is very large, or compressive failure of the base material is governed by plasticity, values $\alpha \leq 1$ become more plausible. Simulations performed by using a lattice model of the base material have shown that α can be lower than 1.0 if heterogeneity and cumulative damage of the base material are considered (Carpinteri et al., 2003). This would explain why, in some cases (usually related to high thrust or to very soft materials), the rate of increase of $\dot{\delta}$ with F_n is more than linear. In any case, the value $\alpha = 1$ corresponds to the (experimentally detected) almost linear dependence of $\dot{\delta}$ on F_n. One should also take into account that the development of wear-flats (with the advancement) provides the progressive increase of the penetration stiffness k (see the next section). From Equation (13), and assuming, as above, that $F_n = n_d f_n$, one obtains:

$$u = \frac{F_n^{1/\alpha}}{(n_d k)^{1/\alpha}} \tag{14}$$

By inserting Equation (14) into Equation (12) one gets:

$$\dot{\delta} = \frac{F_n^{1/\alpha} n_d^{1-1/\alpha} \dot{\varphi}}{2\pi k^{1/\alpha}} \tag{15}$$

which represents the *optimal kinematic functioning point of core drilling*. Equation (15) implies that, if the drilling process is carried out at *constant angular velocity*, the cutting strength of the material does not influence the drilling velocity because a larger resisting torque (in harder materials) is automatically balanced by a larger power absorption ($\dot{\varphi} = P_{mech}/M_t$), provided there is always sufficient supply of mechanical power. Of course, harder materials will require a larger weight on bit to ensure an effective penetration.

The optimal drilling velocity is proportional to the $1/\alpha$-power of the global normal force F_n and inversely proportional to the same power of the penetration stiffness k of a single cutter. Note that the drilling velocity, except for the case when $\alpha = 1$, depends also on the number n_d of active indenters. In particular, in the case $\alpha < 1$ (disordered soft materials, crushing failure), the exponent of n_d in Equation (15) becomes negative, so that

a smaller number of indenters implies a larger drilling velocity. On the contrary, when $\alpha > 1$ (hard homogeneous materials, brittle chipping), the exponent is positive and therefore a larger number of cutters provides better performance. Given two different materials (one much harder than the other), if we attain the same penetration u and the angular velocity $\dot{\varphi}$ is the same, the optimal drilling velocity $\dot{\delta}$ is the same. Of course this corresponds to two different values of F_n and M_t and, more importantly, to different power expenditures.

Let us suppose that each cutter obeys a linear penetration law. From Equation (15), by putting $\alpha = 1$, one obtains:

$$\dot{\delta} = \frac{F_n}{k}\frac{\dot{\varphi}}{2\pi} \tag{16}$$

which tells us that, once the angular velocity is fixed, the drilling velocity is directly proportional to the global normal force F_n, and inversely proportional to the indentation stiffness k of a single cutter. With a linear penetration law, the drilling velocity is not dependent on the number of active cutters. However, when impregnated segments are used, the number of active indenters increases (almost linearly) with the normal force F_n because of their different protrusion from the matrix (Borri-Brunetto et al., 2003). Therefore, a parabolic (global) penetration law can be suggested:

$$F_n = ku^2 \tag{17}$$

where k is a parameter depending on the material characteristics and also on the distribution of indenters over the segments (more specifically, on their concentration and on their elevation distribution). In this case, the drilling velocity depends on the square root of the number of active indenters. Inserting, in fact, the quadratic penetration law (17) into Equation (15), we obtain:

$$\dot{\delta} = \frac{\sqrt{F_n}}{\sqrt{k}}\sqrt{n_d}\frac{\dot{\varphi}}{2\pi} \tag{18}$$

Coupling Kinematics and Mechanics: Definition of the Drilling Strength

Electrical engines can balance larger torques, at fixed angular velocity, by increasing the mechanical power supplied to the bit. The characteristic curves of the engine permit to express the dependence of P_{mech}/M_t on the angular velocity, $\dot{\varphi}$. Beyond a certain value of the resisting torque, however, the engine attains the maximum power, and the regime turns to (almost) constant power control. Further increase of the resisting torque (provided,

e.g., by increasing the normal thrust) implies the decrease of the angular velocity (the extreme condition $\dot{\varphi} = 0$ is the so-called *clogging* condition). To obtain a complete description of the drilling process, the kinematic functioning point must therefore be associated to a mechanical functioning point.

To define a mechanical functioning point, we need to balance the work provided by the engine with the work dissipated by removing the base material through the cutting action. The core drilling process in quasi-brittle materials, like rock, concrete, and masonry, involves different sources of energy expenditure. In particular, frictional energy dissipation with considerable heat production occurs, and secondary processes, like fragmentation and milling, also contribute to the total amount of dissipated energy. The precise determination of each contribution is awkward, since it depends on the geometrical characteristics of the cutter, on the activated friction, on the flushing liquid, and also on the operating conditions (e.g., normal thrust and angular velocity).

Therefore, the simplest way to proceed is to collect all the sources of energy expenditure into a single quantity, S, called *drilling strength*, defined as the energy required to remove the unit volume of the base material during a certain drilling process (Teale, 1965). According to this 'global' definition, the drilling strength is measured in J/m^3, or N/m^2, therefore S has the same physical dimensions of the material's strength σ_u and Young's modulus E. As a first approximation, in fact, the drilling strength S of a certain material can be considered as proportional to its ultimate (crushing) stress σ_u. However, since the drilling strength S depends on the size and shape of the indenters, it is not a material constant, but undergoes remarkable size effects (see below).

As shown in Figure 7, the drilling strength can be related to the cutting force f_t. By equating the work done by the cutting force f_t to the work

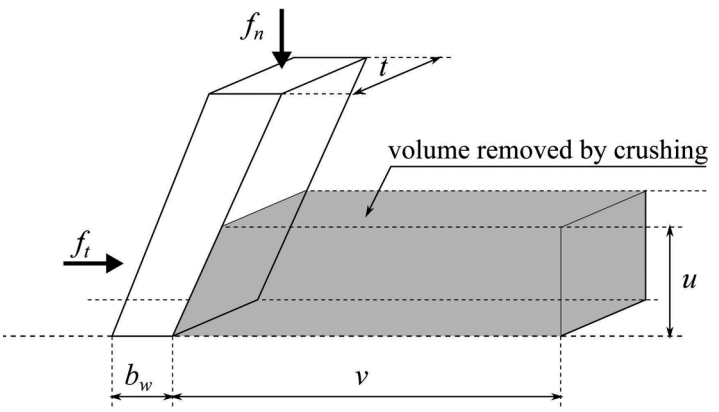

FIGURE 7 Simple crushing model for the indenter cutting action.

dissipated by crushing during an advancement v of the cutter, one obtains the cutting force simply as:

$$f_t = Sut \tag{19}$$

Single-scratch tests carried on large hard cutters ($t = 4\,\text{mm}$), have shown that the drilling strength to be used in the formula is one order of magnitude larger than the usual material's compressive strength (e.g., $S \approx 400\,\text{MPa}$ for a reference concrete). A significant size effect is thus encountered in the cutting process. In the case of impregnated segments, in fact, where the size of the indenting diamonds is much smaller ($t \approx 100\,\mu\text{m}$) the measured drilling strength is close to 1000 MPa. As expected, larger indenters activate less specific strength. This should be kept in mind in the design of core drilling tools.

Another quantity that can be used as a measure of energy expenditure is the so-called *pseudo-friction coefficient* $\mu^* = F_t/F_n$. The drilling strength can be related to μ^* by simple balance arguments. The mechanical power provided by the engine can be expressed by means of the active torque, as a linear function of μ^* or as a linear function of S:

$$M_t\dot{\varphi} = \mu^* F_n R\dot{\varphi} = SA_{bit}\dot{\delta} \tag{20}$$

where $A_{bit} = 2\pi Rt$ is the circular projected area of the groove. Comparing the two formulations, using also Equation (16) one obtains:

$$\mu^* = \frac{St}{k} \tag{21}$$

i.e., the pseudo-friction coefficient can be expressed as a function of the drilling strength and of the penetration stiffness. For instance, by considering the experimental values $S = 350\,\text{MPa}$, $t = 5\,\text{mm}$ and $k = 4.0\,\text{N}/\mu\text{m}$, one gets: $\mu^* = 0.44$, which is a reasonable value for a medium-worn indenter. Equation (21) permits to relate the general kinematic model of drilling to the simpler Coulomb approach, based on the pseudo-friction coefficient $\mu^* = F_t/F_n$ (Davim and Monteiro Baptista, 2000).

Having defined the drilling strength S, we can now couple the kinematic description of the drilling process with the mechanical balance equation. By equating the externally supplied mechanical power P_{mech} to the power dissipated by crushing the base material, one obtains:

$$\eta P_{mech} = SA_{bit}\dot{\delta} \tag{22}$$

where η represents the mechanical efficiency of the engine. From Equation (22), the *mechanical functioning point* is given by:

$$\dot{\delta} = \frac{\eta P_{mech}}{S\ 2\pi Rt} \tag{23}$$

It is important to stress again that the value of S in the balance equation is not an intrinsic property of the base material, but depends on the complex interaction of the cutters with the tool (e.g., it depends on the back rake angle, on the size of the indenters, on the flushing action and on the relative velocity of the cutting edges).

By equating Equations (15) and (23), *the coupled equation of core drilling* is obtained, where the kinematic and mechanical conditions are merged:

$$\frac{F_n^{1/\alpha} n_d^{1-1/\alpha} \dot{\varphi}}{2\pi k^{1/\alpha}} = \frac{\eta P_{mech}}{S\ 2\pi Rt} = \dot{\delta} \tag{24}$$

The above equation can be specialized for different base materials and for different wear states as discussed in the following sections. If the characteristic curve of the engine is known, all the regimes of drilling can be described. For instance, one can deduce the following relation for the mechanical power required to maintain a fixed drilling velocity under a certain thrust force F_n:

$$P_{mech} = \frac{F_n^{1/\alpha} n_d^{1-1/\alpha} \dot{\varphi} SRt}{\eta k^{1/\alpha}} \tag{25}$$

The maximum normal thrust (corresponding to the *clogging* limit) can be computed as a function of the maximum mechanical power (or, equivalently, of the maximum torque $M_{t,max}$):

$$F_{n,max} = k\left(\frac{\eta P_{mech,max}}{SRtn_d^{1-1/\alpha}\dot{\varphi}}\right)^{\alpha} = k\left(\frac{\eta M_{t,max}}{SRtn_d^{1-1/\alpha}}\right)^{\alpha} \tag{26}$$

In addition, the drilling strength corresponding to a certain drilling process can be calculated *a posteriori* from the experimental tests as:

$$S = \frac{\eta P_{mech} k^{1/\alpha}}{F_n^{1/\alpha} n_d^{1-1/\alpha} \dot{\varphi} Rt} = \frac{\eta M_t k^{1/\alpha}}{F_n^{1/\alpha} n_d^{1-1/\alpha} Rt} = \frac{\mu^* \eta k^{1/\alpha}}{F_n^{1/\alpha - 1} n_d^{-1/\alpha} t} \tag{27}$$

The above equation shows that, when $\alpha < 1$, if the minimum drilling strength is pursued, the number of cutters must be as small as possible. The opposite conclusion applies to $\alpha > 1$. Moreover, Equation (27) shows also how, if all the other parameters are fixed, a larger thrust implies a smaller specific consumption of energy (i.e., a better efficiency), consistently with several experimental observations (see, e.g., Miller and Ball, 1990, 1991).

As a final remark, it is worth to remind that the cutting force has been related to the drilling strength S by means of Equation (19). This simple approach permits to consider all the energy dissipation occurring in the

drilling process by means of a single quantity. More refined studies, at the level of the indenters, should permit to estimate the value of S on the basis of theoretical arguments.

Fracture Mechanics Effects on the Drilling Strength

The physical dimensions of the drilling strength S ($[F][L]^{-2}$) correspond to the assumption of crushing (plastic) collapse ahead of the cutter. When brittle fracture, rather than plastic ploughing, governs the collapse of the material, a more appropriate parameter should be used, namely, the fracture toughness K_{IC}, with the anomalous non-integer dimensions $[F][L]^{-3/2}$. Dimensional analysis, in this case, provides:

$$f_t = K_{IC}\rho t u^{1/2} \tag{28}$$

where ρ is a non-dimensional shape factor. Rearranging Equation (24), we obtain the following alternative expression of the drilling velocity:

$$\dot{\delta} = \left(\frac{F_n}{k}\right)^{\frac{1}{2z}} n_d^{-\frac{1}{z}} \frac{P_{mech}}{2\pi R K_{IC}\rho t} \tag{29}$$

where it can be noticed that the dependence of $\dot{\delta}$ on the normal force F_n is weaker than in the case of plastic collapse.

The above description, based on Fracture Mechanics, permits us to also give theoretical basis to the measured size effects on cutting strength, as already pointed out in a previous article by Chiaia (2001). Let us consider two different indenters, pushed into the base material by different values of the normal force (Figure 8). Of course, two different values of the cutting force f_t are induced by the two situations. It is physically plausible to assert that *self-similarity* holds in the distribution of the fragments removed by the ploughing indenters (Carpinteri et al., 2003). The similitude is supported by the power-law distributions of fragments obtained in drilling experiments (Turcotte, 1989). Thereby, assuming the penetration u as the reference length scale, the volume V_f of the removed chip scales as u^3, while the area of the fracture surface A_f scales as u^2.

The drilling strength S has been introduced in the model as a scale-independent parameter. Indeed, when the chipping process is discontinuous, the failure criterion must be written in terms of the stress-intensity factor K_I, to be compared with the fracture toughness of the material, K_{IC}. Thus, the cutting force f_t has to obey the following relation:

$$K_I = \frac{f_t}{\chi u^{3/2}} f(x, y, z) = K_{IC} \tag{30}$$

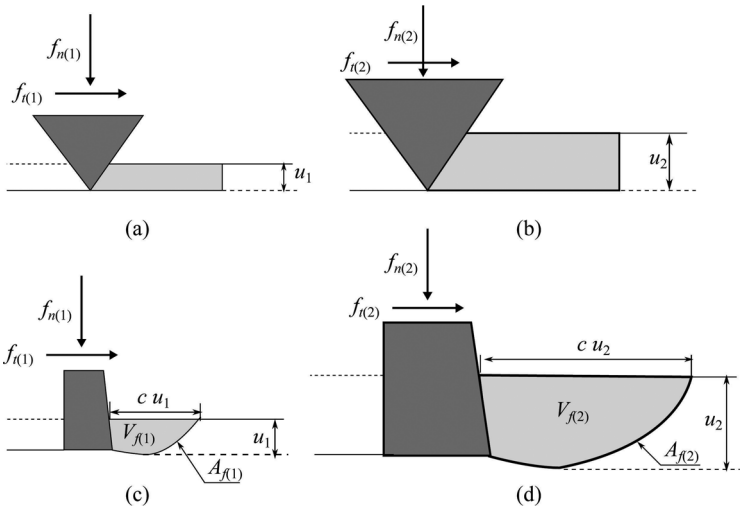

FIGURE 8 Geometrical similarity in a continuous crushing process (a), (b), and in a discontinuous brittle chipping process (c), (d). The similarity postulates that the size of the removed chip is proportional to the penetration of the cutter.

where χ is a non-dimensional geometrical factor, and $f(x,y,z)$ is a non-dimensional geometrical function.

Dimensional analysis yields, in this case, the following scale dependence of the cutting force on the penetration: $f_t \propto u^{3/2}$. This scaling law can also be justified by the dimensional disparity inherent to the energy balance. The elastic strain energy stored in the fragment, in fact, scales as u^3, whereas the energy that can be dissipated along the fracture surface scales as u^2. In the case of plastic crushing, instead, both energies would scale as u^3. The intrinsic nonlinearity of chipping (which is independent of the penetration law) implies that a Coulomb-like linear relation is misleading. It has been observed, in typical drilling experiments (see, e.g., Mishnaevsky 1994, 1995), that the ratio f_t/f_n increases with u. Due to geometrical self-similarity of chips, one can assert that the work W done by the cutting force when removing a single fragment is given by the product of the force times a displacement: cu (Figures 8c and 8d). Therefore, recalling Equation (30):

$$W = f_t cu \propto u^{5/2} \tag{31}$$

where c is a non-dimensional geometrical factor. From Equation (31), one obtains the following scaling law for the drilling strength:

$$S = \frac{W}{\kappa u^3} \propto \frac{1}{\sqrt{u}} \tag{32}$$

where κ is a non-dimensional geometrical factor.

The scaling law of Equation (32) is reminiscent of analogous size-scaling laws found in several fields of strength of materials. If brittle chipping is the main destructive mechanism, the nominal drilling strength S decreases with the penetration u or, which is equivalent, with the size of the indenter, according to a square-root power law. Thus, bigger indenters are more efficient cutters (i.e., they dissipate less energy in chipping), although a larger normal force will be needed to ensure their penetration. These considerations should be taken into account when designing drilling tools. The square-root scaling law is modified in the presence of soft materials, because a certain extent of crushing always occurs immediately ahead of the indenter, and thus the two destruction mechanisms, namely, the plastic and the brittle one, interact with each other (Van Kesteren, 1995).

EMPIRICAL ANALYSIS OF THE WEAR EFFECTS

The most important effect of the development of the wear-flat area is to modify the penetration law. It has been reported (Glowka, 1989) that the penetration force f_n imposed on a worn cutter at a given cut depth is nearly proportional to the wear-flat area in contact with the base material [see also Equation (3a)]. As a first approximation (the exponent α in Equation (13) is kept constant), we can model the evolution of the penetration stiffness according to:

$$k(\delta) = k_0 + C_1 A_w(\delta) \tag{33}$$

where k_0 is the initial penetration stiffness (i.e., corresponding to a virgin, sharp cutter), A_w is the wear-flat area, function of the advancement δ, and C_1 is a constant to be determined experimentally. The rate at which A_w grows with the advancement depends on the mechanical characteristics of the base material but also on the drilling operative parameters (e.g., rotational speed, normal thrust, flushing liquid, see Nabhani, 2001). The following asymptotic law can be proposed:

$$A_w(\delta) = A_{w,max}\left(1 + \frac{C_2}{\delta}\right)^{-\frac{1}{2}} \tag{34}$$

where $A_{w,max}$ is the maximum asymptotic value of the wear-flat area, which is characteristic of the specific cutter, and C_2 is another constant, with the dimension of length, to be determined experimentally. By inserting Equation (34) into Equation (33), the following wear-dependent penetration stiffness is obtained:

$$k(\delta) = k_0 + C_1 A_{w,max}\left(1 + \frac{C_2}{\delta}\right)^{-\frac{1}{2}} \tag{35}$$

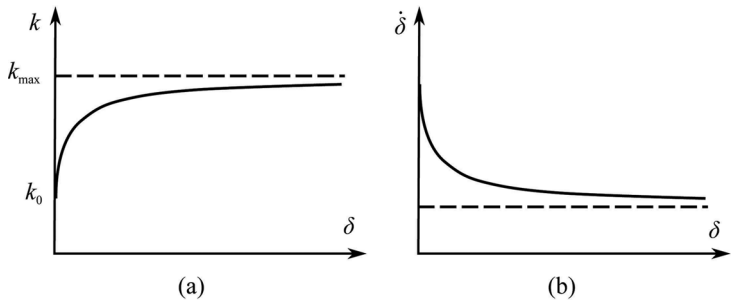

FIGURE 9 Dependence of the penetration stiffness k on the formation of the wear-flat area in drilling, according to Equation (35) (a). Decrease of the drilling velocity due to progressive wear-flat formation, according to Equation (38) (b).

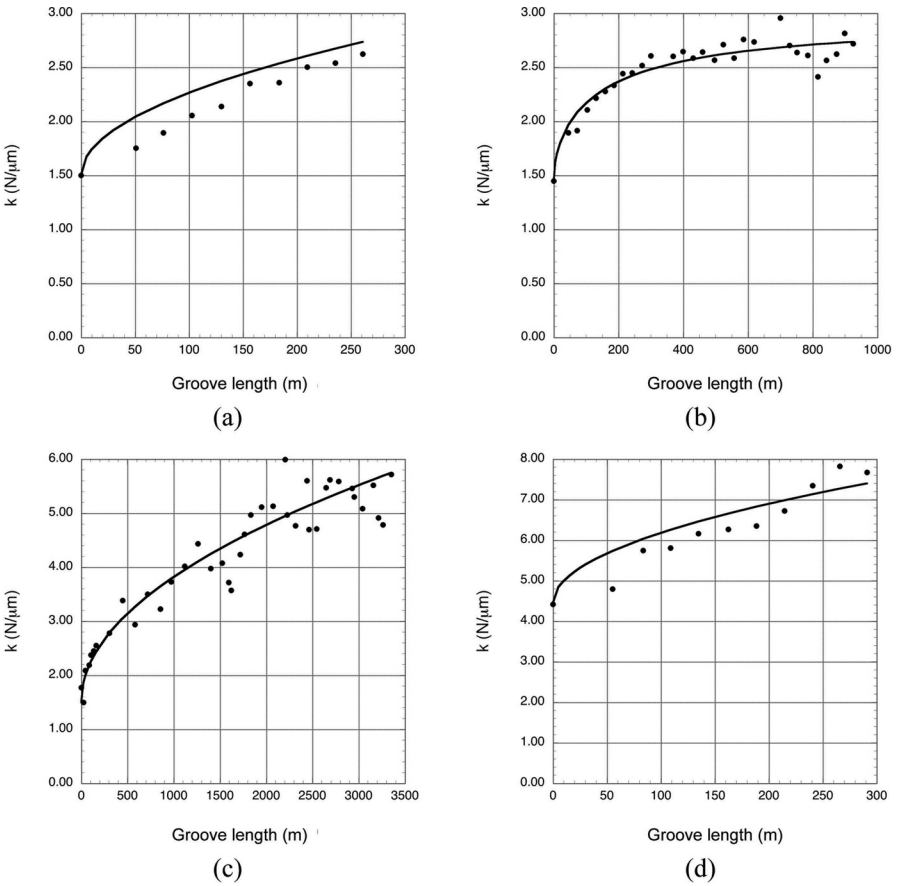

FIGURE 10 Example of measured single scratch test data (dots), for a given cutter configuration, with the best fit of Equation (35) (continuous line), for $\beta = -20^\circ$ (a), -10° (b), 0° (c), $+10^\circ$ (d).

The function in Equation (35), whose graph is depicted in Figure 9a, can be inserted in the drilling formulae, which become wear-dependent. For instance, the decrease of the drilling velocity, due to progressive wear-flat formation at the indenters' edges, is shown in Figure 9b.

The nonlinear Levenberg–Marquardt algorithm, which is based on the least-squares method, can been used to fit Equation (35) to experimental data. For example, some results from single scratch tests with different rake angles are shown in Figure 10. The measurements were made with a single-cutter lathe (Moseley et al., 2009). In these tests, the indenter ploughs a helical groove on the side of the cylinder, with fixed pitch and depth of cut. In all cases the penetration of the cutter (PCD at different rake angles) was kept constant at 100 μm.

If we plot the asymptotic penetration stiffness k_{max} obtained from these experiments, vs. the rake angle, an interesting trend can be evidenced (Figure 11): positive rake angles require larger normal indenting forces to keep the required penetration $u = 100\,\mu\text{m}$, and accordingly, the larger the rake angle, the larger the asymptotic value of k. The conclusion that would be drawn from these very limited data is that cutters with positive or null rake angle, although activating a smaller value of the drilling strength, are more sensitive to wear, compared to cutters with negative rake angle.

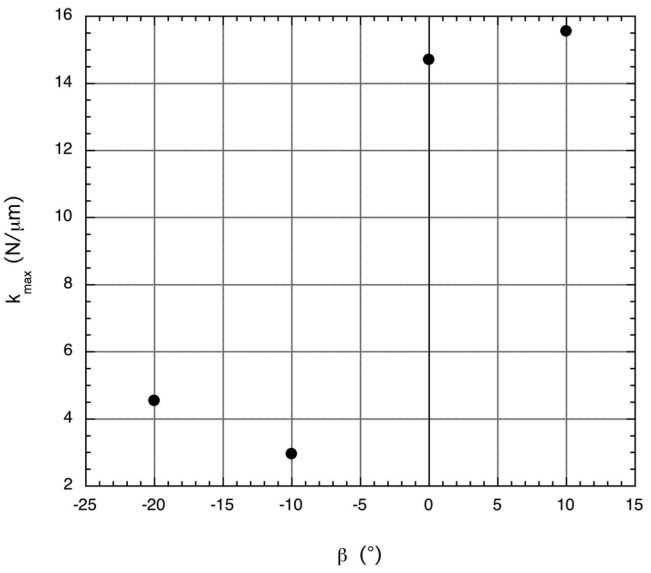

FIGURE 11 Asymptotic penetration stiffness k_{max} as a function of the rake angle from the data in Figure 10.

THE GLOBAL EQUATION OF CORE DRILLING: ROLE OF THE RAKE ANGLE AND CLOGGING LIMIT

The dependence of the drilling strength S on the back rake angle can be expressed by relating the helicoidal theory of core drilling to the geometrical configuration of the single cutter. This dependence is explicitly taken into account by the static balance proposed by Wojtanowicz and Kuru (1993), although, in that theory, the cutting mechanism is restricted, whatever the back rake angle, to plastic crushing.

Considering the balance Equations (3), and expressing the drilling strength S as the work of the cutting force per unit of removed volume along the scratch [see also Equation (19)], we obtain an expression where S can be related to a reference drilling strength S^* measured for $\beta = 0$:

$$S(\beta) = S^* \frac{\mu \cos\beta - \sin\beta}{\mu} \tag{36}$$

Notice that the trigonometric term $(\mu \cos\beta - \sin\beta)$ was already present in the drillability constant K [Equation (9)], as defined by Wojtanowicz and Kuru (1993). In Figure 12, a plot of the ratio S/S^* is shown for the case $\mu = 0.5$. Therefore, positive rake angles imply a lower apparent drilling strength, i.e., a better drillability. It is important to remind, however, that the above formula, which is based on simple static balance laws, has to be considered as valid only in a limited range of angles $(-10° < \beta < 10°)$,

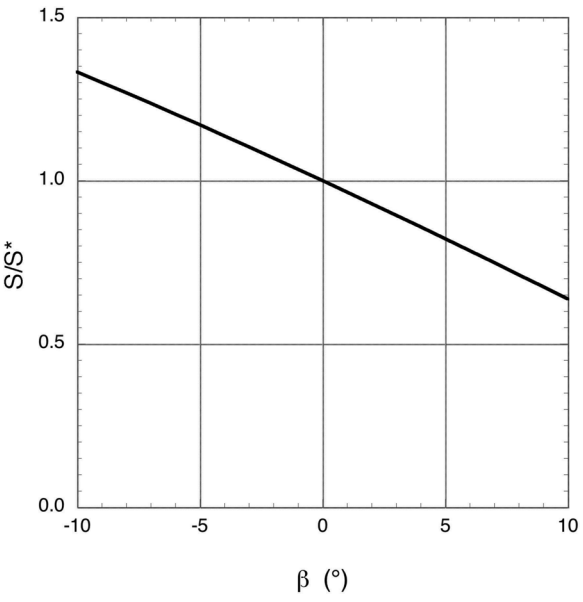

FIGURE 12 Influence of the back rake angle on the apparent drilling strength.

because larger values of β imply different rupture mechanisms ahead of the cutters. By inserting Equation (36) in the drilling model [Equation (24)], the dependence of the drilling equation on the back rake angle β is made explicit:

$$\frac{F_n^{1/\alpha} n_d^{1-1/\alpha} \dot{\varphi}}{2\pi k^{1/\alpha}} = \frac{\eta P_{mech}}{S^* \frac{\mu\cos\beta - \sin\beta}{\mu} 2\pi R t} = \dot{\delta} \tag{37}$$

The above relation shows that the drilling velocity is larger for positive back rake angles. If also the formation of the wear-flat area is considered [Equation (35)], one obtains the *global equation of core drilling*:

$$\frac{F_n^{1/\alpha} n_d^{1-1/\alpha} \dot{\varphi}}{2\pi \left[k_0 + C_1 A_{w,max} \left(1 + \frac{C_2}{\delta}\right)^{-\frac{1}{2}} \right]^{1/\alpha}} = \frac{\eta P_{mech}}{S^* \frac{\mu\cos\beta - \sin\beta}{\mu} 2\pi R t} = \dot{\delta} \tag{38}$$

From this equation, all the drilling regimes can be modelled provided the characteristic curve of the engine is known. In addition, one can also estimate the influence of wear on the critical normal force $F_{n,max}$, which was previously defined as the *clogging force* by means of Equation (26). A minimum value of the normal force is needed to ensure cutting, even with sharp virgin indenters, otherwise only polishing of the concrete surface occurs. This peculiar behavior contradicts the classical theories of elastic indentation, since at the apex of a sharp indenter an infinite pressure is known to exist, which would immediately originate plasticization or cracking. Experiments on marble and limestone showed that the surface effect is important at scales below 100 μm (see, e.g., the results described by Mancini et al., 1993).

During the drilling process, a stationary regime is sought, to which an approximately constant angular velocity $\dot{\varphi}$ corresponds. This means that, if the normal thrust is increased, the resisting torque increases but the engine automatically increases the power supply and the ratio P_{mech}/M_t remains constant. After a certain value, there is no more possibility to increase the mechanical power. Thus, a new regime comes into play, where P_{mech} is approximately constant. Thereby, if the user increases the thrust, the only possibility to compensate the increase of M_t is that the angular velocity decreases.

This implies that, in this regime, the drilling velocity is inversely proportional to F_n whatever the hypothesis made for material removal. For very high values of M_t, clogging occurs, and the velocity suddenly goes to zero. Once the maximum torque (or the maximum mechanical power) is fixed, one notes that $F_{n,max} \propto k(\delta)$, thus the clogging limit increases with wear. At the same time, S increases due to wear-flat formation and the maximum rate of advancement decreases [see the second term in Equation (38)]. In conclusion, due to wear-flat formation, the clogging point C follows the curve CC_I, as depicted in Figure 13.

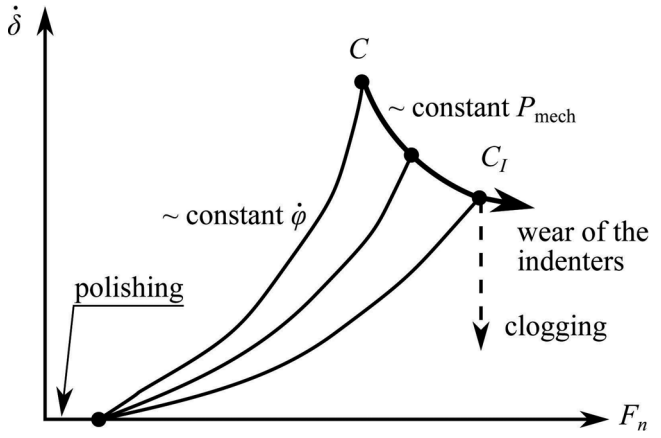

FIGURE 13 Influence of wear on the characteristic curve (drilling velocity vs. thrust).

Equation (38) represents a rather general formulation for rotary drilling. The above formula should be compared to drilling experiments in order to assess its validity and fit the various parameters (α, k_0, μ, A_w, C_1, and C_2) to real situations. Once the empirical constants related to the wear properties of the indenter (and to the abrasive properties of the base material) are determined, all the quantities involved in a drilling process can be calculated by means of Equation (38).

As an example, we apply the model to find *a priori* the drilling strength S^* that is encountered during a hypothetical drilling process with a core bit. We can use, for instance, the following data, for a core bit with three large used cutters: $P_{mech} = 2600\,\text{W}$, $F_n = 1400\,\text{N}$, $n_d = 3$, $\beta = -5^\circ$, $\dot{\varphi} = 415\,\text{rpm}$, $R = 102\,\text{mm}$, $t = 4\,\text{mm}$. In addition, according to typical specifications, we assume $\eta = 0.7$ as the efficiency of the engine. As a first approximation, let us neglect the wear-flat formation and let us choose a linear penetration law, i.e., $\alpha = 1$. We assume the value $k = 4.5\,\text{N}/\mu\text{m}$, which is reasonable for a traditional concrete, with characteristic compressive strength $f_{ck} = 50\,\text{MPa}$. This value corresponds to an average penetration of the indenters $u = 104\,\mu\text{m}$ and can be considered as a representative value for a medium wear-flat formation.

According to these values, the model provides $S = 345\,\text{MPa}$. The reference drilling strength of the base material, which would be activated by a tool with back rake angle $\beta = 0^\circ$, would be lower: $S^* = 294\,\text{MPa}$. Notice that the value which was calculated *a posteriori* through calculation of the removed volume in a test conducted at the Politecnico di Torino [i.e., by inserting the measured experimental drilling velocity into Equation (38)], was equal to $S = 370\,\text{MPa}$. There is thus a good correspondence between the theory and the experiments, which could be further improved

by taking into account the real penetration law ($\alpha \neq 1$) and the effect of wear-flat formation. Notice also that the value $S = 345$ MPa is considerably lower than the drilling strength that is currently measured in classic core drilling by impregnated bits. We expected this in the presence of large indenters, due to size-effects and because comminution and milling effects are substantially reduced.

CONCLUSIONS

In this article, the drilling model by Wojtanowicz and Kuru (1993), based on the balance of the forces acting on a cutter, has been supplemented by an original kinematic approach, which takes into account the helicoidal nature of the groove. Consideration of a kinematic constraint on steady-state drilling operations permits to find the optimal drilling velocity, defined by Equation (15), as a function of the tool parameters and the thrust applied to the core bit.

If the drilling strength S is introduced, the purely kinematic description of the drilling process can be coupled with the mechanical balance equation, after having obtained the drilling velocity corresponding to the mechanical functioning point (Equation (23)).

The resulting coupled equation of core drilling (Equation (24)) groups the parameters of the tool and the response of the drilled material, and allows one to evaluate the expected performance of the tool. By using this equation, the influence of tool wear on the drilling velocity can be shown, and different drilling regimes can be described. Moreover, the thrust on the tool corresponding to the clogging limit is evaluated as a function of the parameters of the engine, the core-bit, and the material.

The global equation of core drilling (Equation (38)) takes into account also the tool's wear state (i.e., wear-flat formation, variation of the penetration stiffness). It has been shown also, by means of the proposed model, how the drilling strength can be estimated on the basis of measurable mechanical and geometrical parameters.

NOMENCLATURE

A_{bit}	projected circular area of the groove
A_c	cutting area
A_f	area of chip fracture surface
A_w	wear-flat area
C	non-dimensional chip length
C_1, C_2	best fit parameters of the wear law
E	Young's modulus of the base material

F_n	total thrust force on bit (weight on bit)
F_t	total tangential force on cutters
K	drillability constant
K_1	stress intensity factor
K_{IC}	fracture toughness of the base material
M_t	torque on bit
P_{mech}	mechanical power supplied by the engine
R	radius of the core bit
S	drilling strength of the base material
S^*	drilling strength for $\beta = 0$
S_c	crushing resistance of the base material
S_w	penetration resistance of the base material
U_D	empirical wear function
V_b	removed volume of base material
V_f	volume of the chip
W	work of the cutting force for chip removal
f_c	cutting force on cutter (orthogonal to the cutting area)
f_{ck}	characteristic compressive strength
f_{fc}	frictional force on the cutting area
f_{fw}	frictional force on the wear-flat
f_h	horizontal force on cutter
f_n	normal force on cutter
f_t	tangential force on cutter
f_w	force orthogonal to the wear-flat
k	penetration stiffness of a single cutter
k_0	penetration stiffness of a virgin cutter
k_{max}	asymptotic penetration stiffness
k_1, k_2, k_3, k_4, k_5	empirical constants
n_d	number of cutters on the core bit
s	circumferential spacing of the cutters
t	width of the cutters
u	penetration of the indenter in the base material
v	advancement of cutters in the tangential direction
α	exponent of the penetration law for a single cutter
β	back rake angle of cutters
δ	drilled distance in the axial direction
$\dot{\delta}$	drilling velocity (rate of penetration)
η	efficiency of the engine
$\dot{\varphi}$	angular velocity of the core bit
κ, χ	non-dimensional shape factors
λ	side rake angle of cutters
μ	sliding friction coefficient between cutter and base material
μ^*	pseudo-friction coefficient
σ_u	ultimate strength of the base material
θ	cutting angle (slope of the helicoidal trajectory)
$\bar{\theta}$	optimal cutting angle

REFERENCES

Borri-Brunetto, M.; Carpinteri, A.; Invernizzi, S. (2003) Characterization and mechanical modeling of the abrasion properties of sintered tools with embedded hard particles. *Wear*, 254: 635–644.

Carpinteri, A.; Chiaia, B.; Invernizzi, S. (2003) Numerical analysis of indentation fracture in quasi-brittle materials. *Engineering Fracture Mechanics*, 71(4–6): 567–577.

Chiaia, B. (2001) Fracture mechanisms induced in a brittle material by a hard cutting indenter. *International Journal of Solids and Structures*, 38(44–45): 7747–7768.

Davim, J.P.; Monteiro Baptista, A. (2000) Relationship between cutting force and PCD cutting tool wear in machining silicon carbide reinforced aluminium. *Journal of Materials Processing Technology*, 103(3): 417–423.

Fischer-Cripps, A.C. (2000) *Introduction to Contact Mechanics*. Springer Verlag, New York.

Glowka, D.A. (1989) Use of single-cutter data in the analysis of PDC bit designs: part 1—development of a PDC cutting force model. *Journal of Petroleum Technology*, 41(8): 797–849.

Hanna, I.S. (2000) Selection and evaluation of polycrystalline diamond compact (PDC) bits. *Saudi Aramco Journal of Technology*, Winter 1999/2000: 53–69.

Kerr, C.J. (1988) PCD drill bit design and field application evolution. *Journal of Petroleum Technology*, 40(3): 327–332.

Mancini, R.; Cardu, M.; Fornaro, M.; Linares, M. (1993) Scale effects in the 'micro-scale' rock mechanics problems. In A. Pinto da Cunha (ed.), *Scale Effects in Rock Masses 93—Proceedings of the Second International Workshop on Scale Effects in Rock Masses*, Balkema, Rotterdam, pp. 151–158.

Mellor, M. (1976) Mechanics of cutting and boring. Part II: Kinematics of axial rotation machines. Report 76–16, *Cold Regions Research and Engineering Laboratory*, Hanover, New Hampshire, USA.

Miller, D.; Ball, A. (1990) Rock drilling with impregnated diamond microbits—An experimental study. *International Journal of Rock Mechanics and Mining Sciences & Geomechanics Abstracts*, 27(5): 363–371.

Miller, D.; Ball, A. (1991) The wear of diamonds in impregnated diamond bit drilling. *Wear*, 141(2): 311–320.

Mishnaevsky, L.L. (1994) Investigation of the cutting of brittle materials. *International Journal of Machine Tools and Manufacture*, 34(4): 499–505.

Mishnaevsky, L.L. (1995) Physical mechanisms of hard rock fragmentation under mechanical loading: a review. *International Journal of Rock Mechanics and Mining Sciences*, 32(8): 763–766.

Moseley, S.G.; Bohn, K.-P.; Goedickemeier, M. (2009) Core drilling in reinforced concrete using polycrystalline diamond (PCD) cutters: Wear and fracture mechanisms. *International Journal of Refractory Metals & Hard Materials*, 27: 394–402.

Nabhani, F. (2001) Wear mechanisms of ultra-hard cutting tools materials. *Journal of Materials Processing Technology*, 115(3): 402–412.

Sneddon, M.V.; Hall, D.R. (1988) Polycrystalline diamond: manufacture, wear mechanisms, and implications for bit design. *Journal of Petroleum Technology*, 40(12): 1593–1601.

Teale, R. (1965) The concept of specific energy in rock drilling. *International Journal of Rock Mechanics and Mining Sciences*, 2(1): 55–73.

Turcotte, D. (1989) Fractals in geology and geophysics. *Pure and Applied Geophysics*, 131(1–2): 171–196.

Van Kesteren, A. (1995) Numerical simulations of crack bifurcation in the chip forming cutting process in rock. In: Baler, G.; Karihaloo, B.L., (editors), *Fracture of Brittle Disordered Materials*, E. & F. N. Spon, London; 505–524.

Wojtanowicz, A.K.; Kuru, E. (1993) Mathematical modelling of PDC bit drilling process based on a single cutter mechanics. *Journal of Energy Resources Technology, Transactions of the ASME*, 115(4): 247–256.